CLOSE TRAVERSE WITH TOTAL STATION IN A CALIBRATION BASELINE USING DIFFERENT REFLECTIVE SURFACES

Isaac Ramos Junior, Andrea de Seixas, Sílvio Jacks dos Anjos Garnés
Department of Cartographic Engineering, Federal University of Pernambuco, 50670-901, Recife, Brazil
isaac.ramos@ufpe.br
andrea.seixas@ufpe.br
silvio.jacks@ufpe.br

ABSTRACT

This article examines three different traverses, measured with three different types of reflective surfaces, of a calibration baseline at the Recife campus of the Federal University of Pernambuco, Brazil. The baseline, which has seven pillars, labeled with P1 to P7, with forced centering devices, has a slight misalignment that made the traverse analysis possible. Due to this, it was used a close traverse formed by the pillar sequence P1, P3, P4, P7, P6, P5, P2, P1, opening up the possibility for various types of comparisons. Field data were first subjected to preliminary statistical analysis, and after that, the traverses calculations were made using the least square method. After that, three comparisons were made using one of the targets as reference, referring to angles, distances and coordinates. No cases were found in which differences between quantities exceeded significantly those predicted by least squares estimates. The next step was to use the adjusted coordinates of the reference target to calculate the distances between the pillars, in pairs, so that they could be compared with previous work. This comparison was made, and the largest difference between the distances was -2.2 mm, which is not beyond the estimated linear precision for any of the distances involved. Furthermore, among future works, it is recommended that high-precision geometric leveling of the base be carried out, so that the vertical component can be studied.

KEYWORDS: *Geodetic Engineering, Metrology, Precise Instrumentation.*

I. INTRODUCTION

The total station integrates an electronic theodolite, an electronic distance measuring device, and a microprocessor with a memory unit. This instrument is designed for measuring horizontal and slope distances, horizontal and vertical angles, and elevations in topographic surveys, in geodetic works, as well as for other survey applications [1,2]. Total stations advanced into robotic total stations (RTS), incorporating various extra features such as motion-controlling actuators, cameras, and tracking software. These enhancements allow them to operate independently, either by adhering to a preloaded measurement program or by being directed via remote control [3].

A common approach for integrating RTS measurements is by using a traverse. A traverse is a method for establishing horizontal control by determining the rectangular coordinates of a series of control points situated around a site, using a combination of angle and distance measurements [4].

Before taking further measurements at the instrument point, it is essential to complete traverse observations. This allows future measurements to be linked to the traverse, even if the instrument is moved. Traverses can be closed to detect any errors, enabling the calculation of the vector sum. Discrepancies can be checked for errors, and adjustments can be made if needed [5].

A baseline is a spatial line defined by a set of permanent aligned points with a precise distance. These points, known as baseline points, typically consist of elevated pillars above ground. Often, the term "length baseline" refers to multiple outdoor baseline points and is primarily used to calibrate the additive and other constants of distance-measuring instruments like total stations [6], but other synonymous can

be found for length baseline, such as geodetic calibration baseline [7], baseline [8], electronic distance measuring instrument (EDMI) calibration baseline [9] or calibration baseline [10].
However, from the point of view of technical and scientific research, calibration baselines, even after they are deployed to perform calibrations, have been used to investigate different variables, beyond investigations into the instrumental constants of EDMI's. Thus, for example, [11] studied variations in the length of a calibration baseline in relation to changes in air temperature over time; in [12] there is a research that used a calibration baseline to compare observations made with a total station and a Global Positioning System (GPS) receiver; and in [13] there is a study on the stability of the pillars of a calibration baseline, carried out for different periods.
Besides these, in [14], a slight misalignment of a calibration baseline in Federal University of Pernambuco - Brazil was identified, which can be treated as a closed traverse, composed of pillars P1, P3, P4, P7, P6, P5, P2 and P1. From this specific result, several research hypotheses can be raised. In this context, the hypothesis tested in this work was that, based on three closed traverses, measurements made with a RTS, with three different types of targets (a 360° prism, a circular prism, and a reflective sheet) there are no significant differences between the angles, distances and coordinates of the pillars, when using as a reference the 360° prism, because it is the original target that accompanies the equipment.

II. MATERIALS AND METHODS

The calibration baseline at the Federal University of Pernambuco was implemented in 1990 by the Spatial Metrology Laboratory of the Department of Cartographic Engineering. The pillars were built to allow intervisibility between them, and all of them have a forced centering device [15]. In this study, seven pillars of these calibration baseline were designated with the names P1, P2, P3, P4, P5, P6, and P7, however, because the misalignment, the close traverse sequence used were P1, P3, P4, P7, P6, P5, P2 and P1, as mentioned in item I. Figure 1 depicts the baseline from P7 to P1.

Figure 1. The calibration baseline is composed of seven pillars with forced centering, in June 2024.

The fieldwork was carried out using a Topcon RTS, model GT-605, in fine measurement mode, factory calibrated, configured to collect only horizontal directions and horizontal distances. The equipment has a linear accuracy of ±2mm + 2ppm (parts per million) and an angular accuracy of 5" [16]. Figure 2 shows the equipment installed on one of the baseline pillars.

Figure 2. The Topcon GT-605 RTS used in the measurements, in June 2024.

Three accessories were used as targets: a Topcon 360° prism ATP1, a Geodetic 04S Circular Prism, and a Xpex reflective sheet. As they have different reflective surfaces, each of them was used independently in the baseline, enabling the measurement of three closed traverses that can be compared. Figure 3 shows the three targets used.

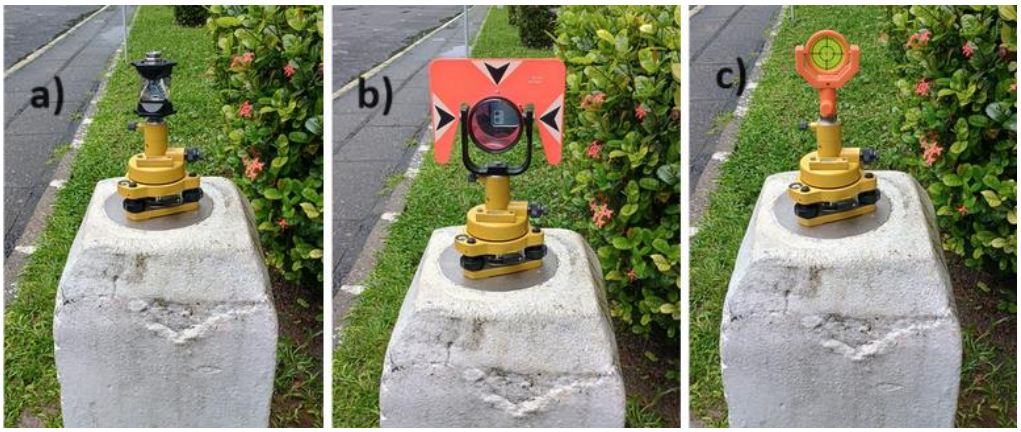

Figure 3. Three different reflective surfaces used as target, in June 2024: a) 360° prism; b) circular prism; and c) reflective sheet.

The first phase of the work consisted of measuring the angles and horizontal distances of the traverse, for each of the targets, accounting for three traverses. For each pillar, the angular measurements and computations were made using the Direction Measurement in Sets [17], as follows: Initially with the telescope in direct position and the circle close to 0°, the targets (backsight and foresight) were observed clockwise in sequence. Next, the telescope was flipped, and all targets were observed in the reverse telescope position and order. This series of measurements is called a set. Then, the circle was shifted by close to 60° and the process was repeated. And then, the circle was shifted again by close to 120° and the process was repeated.

The measurements were carried out starting and ending at pillar 1, traveling along the traverse in a clockwise direction, reading external angles. For each angular reading, a horizontal distance was also collected.

After collecting data in the field, the observations were transferred from the equipment to a computer using a Python program made specifically for this purpose. At this time, from the raw data, the mean angular directions are then adjusted to the starting direction (that is, the zero direction) by subtracting the initial value from all others, and the final directions are obtained by averaging the reduced means of the individual sets. The calculations of means and reduced means were verified with sum checks. These calculations were made using another original Python program, made specifically for this work.

As the angular observations were made for three different types of targets, in different days, after the calculations described above, the results were subjected to the two statistical tests. The first test was the Shapiro-Wilk normality test [18], to check whether observations of each point of the traverse, for each target, belong to a normal distribution; and the statistical t-test to determine if there is a significant difference between the means of the observations sets [18], in pairs, for each pillar. To carry out these

statistical tests, the statistical module of a scientific program called AstGeoTop [19] was used. In relation to horizontal distances, arithmetic averages were calculated for each target, for each pillar.
Once the average of horizontal angles and distances were calculated, and statistical tests were carried out for angles, the data was submitted again to the scientific program AstGeoTop, however, this time to the module planimetric surveying [20], so that the three traverses could be calculated using the least squares method, using the specific program module. The least squares method was chosen because this is the most rigorous adjustment procedure available [21].
After adjustment using the least squares method, the results could be compared. Thus, for each traverse, the horizontal angles, horizontal distances, and the coordinates (X, Y), with their respective precision estimates, were selected and compared, using the traverse with the 360° prism as a reference, as this is the accessory that originally accompanies the equipment.

III. RESULTS AND DISCUSSIONS

The first results were those referring to the Shapiro-Wilk normality test for horizontal angles. All sets of observations, selected for each target and for each pillar were tested, and, after the test, all of them were statistically considered to come from a normal distribution at the 1% significance level, which means that the set of observations for each target and for each pillar were found to be normally distributed with a confidence of 99%. According to [18] results significant at the 1% level are more persuasive and offer stronger evidence against the null hypothesis than those significant at the, for example, 5% level.
The second results referred to the t-test, which analyzed the samples in pairs, for the three types of targets, for each pillar. The results of the t-test are found in tables 1 to 7, below. To carry it out in all cases, a significance level of 1% was used, and a degree of freedom equal to 5, since, for each sample of observations, six angular readings were taken, three in the direct position of the telescope, and three in the inverted position. From the results of the t-test, it can be concluded with a 99% confidence level that in none of the cases do the means have statistically relevant differences, as all t-statistics values are below the t-critical values.

Table 1. T-test results for Pillar 1.

Backsight	Station	Foresight	set	sample	mean	variance	t statistics	t critical	conclusion
P2	P1	P3	1st	360° prism	359°58`57,7"	0°00`00,06441"	0,4342	4,032	do not differ
				circular prism	359°59`01,3"	0°00`00,01007"			
			2nd	360° prism	359°58`57,7"	0°00`00,06441"	0,6525	4,032	do not differ
				reflective sheet	359°58`59,8"	0°00`00,06027"			
			3rd	circular prism	359°59`01,3"	0°00`00,01007"	0,1984	4,032	do not differ
				reflective sheet	359°58`59,8"	0°00`00,06027"			

Table 2. T-test results for Pillar 2.

Backsight	Station	Foresight	set	sample	mean	variance	t statistics	t critical	conclusion
P5	P2	P1	1st	360° prism	179°59`26,3"	0°00`00,01741"	2,2203	4,032	do not differ
				circular prism	179°59`35,2"	0°00`00,00305"			
			2nd	360° prism	179°59`26,3"	0°00`00,01741"	1,3587	4,032	do not differ
				reflective sheet	179°59`33,2"	0°00`00,02638"			

			3rd	circular prism	179°59`35,2"	0°00`00,00305"	0,5806	4,032	do not differ
				reflective sheet	179°59`33,2"	0°00`00,02638"			

Table 3. T-test results for Pillar 3.

Backsight	Station	Foresight	set	sample	mean	variance	t statistics	t critical	conclusion
P1	P3	P4	1st	360° prism	179°59`36,5"	0°00`00,07997"	0,024	4,032	do not differ
				circular prism	179°59`36,7"	0°00`00,00019"			
			2nd	360° prism	179°59`36,5"	0°00`00,07997"	1,0077	4,032	do not differ
				reflective sheet	179°59`31,8"	0°00`00,01082"			
			3rd	circular prism	179°59`36,7"	0°00`00,00019"	1,8681	4,032	do not differ
				reflective sheet	179°59`31,8"	0°00`00,01082"			

Table 4. T-test results for Pillar 4.

Backsight	Station	Foresight	set	sample	mean	variance	t statistics	t critical	conclusion
P3	P4	P7	1st	360° prism	180°01`11,3"	0°00`00,00874"	0,3555	4,032	do not differ
				circular prism	180°01`12,2"	0°00`00,00071"			
			2nd	360° prism	180°01`11,3"	0°00`00,00874"	1,5492	4,032	do not differ
				reflective sheet	180°01`09,3"	0°00`00,01207"			
			3rd	circular prism	180°01`12,2"	0°00`00,00071"	1,1415	4,032	do not differ
				reflective sheet	180°01`09,3"	0°00`00,01207"			

Table 5. T-test results for Pillar 5.

Backsight	Station	Foresight	set	sample	mean	variance	t statistics	t critical	conclusion
P6	P5	P2	1st	360° prism	180°02`13,0"	0°00`00,01711"	2,2328	4,032	do not differ
				circular prism	180°02`19,2"	0°00`00,00427"			
			2nd	360° prism	180°02`13,0"	0°00`00,01711"	0,9682	4,032	do not differ
				reflective sheet	180°02`12,0"	0°00`00,01822"			
			3rd	circular prism	180°02`19,2"	0°00`00,00427"	2,5507	4,032	do not differ
				reflective sheet	180°02`12,0"	0°00`00,01822"			

Table 6. T-test results for Pillar 6.

Backsight	Station	Foresight	set	sample	mean	variance	t statistics	t critical	conclusion
P7	P6	P5	1st	360° prism	179°59`46,2"	0°00`00,00260"	3,4616	4,032	do not differ
				circular prism	179°59`56,5"	0°00`00,00775"			
			2nd	360° prism	179°59`46,2"	0°00`00,00260"	1,0518	4,032	do not differ
				reflective sheet	179°59`47,8"	0°00`00,00494"			
			3rd	circular prism	179°59`56,5"	0°00`00,00775"	2,9942	4,032	do not differ
				reflective sheet	179°59`47,8"	0°00`00,00494"			

Table 7. T-test results for Pillar 7.

Backsight	Station	Foresight	set	sample	mean	variance	t statistics	t critical	conclusion
P4	P7	P6	1st	360° prism	359°58`36,0"	0°00`00,00433"	1,6308	4,032	do not differ
				circular prism	359°58`32,7"	0°00`00,00152"			
			2nd	360° prism	359°58`36,0"	0°00`00,00433"	1,5524	4,032	do not differ
				reflective sheet	359°58`32,8"	0°00`00,00582"			
			3rd	circular prism	359°58`32,7"	0°00`00,00152"	0,0617	4,032	do not differ
				reflective sheet	359°58`32,8"	0°00`00,00582"			

After being accepted in initial statistical tests, the data were subjected to traverse calculations using the least squares method, for each type of target, generating three traverses. In this way, results were obtained for the adjusted observations (angles and horizontal distances), and for the adjusted parameters (plane coordinates), as well as the precision estimate (standard deviation, or s.d) for each of them. For all traverses, coordinates X=1000,000 meters and Y=1000,000 meters for pillar 1, and the azimuth from pillar 1 to pillar 3 was arbitrated in 0°0`00,0" for all traverses, because in this way the coordinates could be compared. The results of the observations adjustment computations are in tables 8 and 9.

Table 8. Results for the adjusted horizontal angles.

Backsight	Station	Foresight	360° Prism		Circular Prism		Reflective Sheet	
			Angle	s.d angle (")	Angle	s.d angle (")	Angle	s.d angle (")
P2	P1	P3	359°59`02,8"	3,0219	359°58`57,9"	3,6870	359°59`02,9"	3,6797
P1	P3	P4	179°59`40,7"	3,2431	179°59`33,8"	3,9570	179°59`34,5"	3,9492
P3	P4	P7	180°01`11,0"	0,5588	180°01`12,1"	0,6819	180°01`09,5"	0,6806
P4	P7	P6	359°58`36,3"	1,1249	359°58`31,8"	1,3725	359°58`33,9"	1,3697
P7	P6	P5	179°59`48,6"	1,7525	179°59`51,0"	2,1382	179°59`52,6"	2,134
P6	P5	P2	180°02`13,9"	1,7926	180°02`18,0"	2,1872	180°02`13,6"	2,1828
P5	P2	P1	179°59`26,6"	2,3448	179°59`35,3"	2,8610	179°59`33,2"	2,8553

Table 9. Results for the adjusted horizontal distances.

Station	Foresight	360° Prism		Circular Prism		Reflective Sheet	
		H. dist (m)	s.d H. dist (m)	H. dist (m)	s.d H. dist (m)	H. dist (m)	s.d H. dist (m)
P1	P3	12,739	0,0025	12,739	0,0029	12,740	0,0030
P3	P4	33,125	0,0025	33,126	0,0029	33,127	0,0030
P4	P7	121,629	0,0026	121,630	0,0029	121,630	0,0030
P7	P6	32,258	0,0025	32,259	0,0029	32,261	0,0030
P6	P5	39,480	0,0025	39,480	0,0029	39,478	0,0030
P5	P2	87,453	0,0026	87,454	0,0029	87,455	0,0030
P2	P1	8,301	0,0025	8,301	0,0029	8,303	0,0030

The results for the parameters adjustment (i.e, for the pillars coordinates) were separated in table 10 for the 360° prism and in table 11 for the other two targets, because the 360° prism was the reference target, as already mentioned. After adjustment, the three polygonals were subjected to a quality control analysis, in which the chi-square test was used to test whether the adjusted observations belong to a normal distribution, at a significance level of 5%. All three were approved.

Table 10. Results for the adjusted coordinates for 360° prism, that was used as reference.

Station	360° Prism			
	X (m)	s.d X (m)	Y (m)	s.d Y (m)
P1	1000,0000	0,0000	1000,0000	0,0000
P3	1000,0000	0,0000	1012,7388	0,0025
P4	999,9969	0,0005	1045,8636	0,0033
P7	1000,0274	0,0024	1167,4924	0,0036
P6	1000,0324	0,0019	1135,2342	0,0036
P5	1000,0407	0,0014	1095,7540	0,0033
P2	1000,0023	0,0001	1008,3008	0,0025

Table 11. Results for the adjusted coordinates for circular prism and reflective sheet.

Station	Circular Prism				Reflective Sheet			
	X (m)	s.d X (m)	Y (m)	s.d Y (m)	X (m)	s.d X (m)	Y (m)	s.d Y (m)
P1	1000,0000	0,0000	1000,0000	0,0000	1000,0000	0,0000	1000,0000	0,0000
P3	1000,0000	0,0000	1012,7389	0,0029	1000,0000	0,0000	1012,7395	0,0030
P4	999,9958	0,0006	1045,8648	0,0038	999,9959	0,0006	1045,8660	0,0039
P7	1000,0229	0,0030	1167,4947	0,0041	1000,0218	0,0030	1167,4955	0,0043
P6	1000,0295	0,0024	1135,2356	0,0041	1000,0284	0,0024	1135,2350	0,0043
P5	1000,0393	0,0017	1095,7555	0,0038	1000,0379	0,0017	1095,7575	0,0039
P2	1000,0025	0,0001	1008,3014	0,0029	1000,0023	0,0001	1008,3030	0,0030

The results above allow for several comparisons. For this work, comparisons were made between horizontal angles, horizontal distances and coordinates, always using the 360° prism as a reference. In

this way, tables 12 to 14 were created, which show the results for the differences obtained for angles, distances and coordinates, respectively.

Table 12. Results for comparing adjusted horizontal angles.

Backsight	Station	Foresight	360° Prism -Circular Prism	360° Prism - Reflective Sheet
P2	P1	P3	4,9"	-0,1"
P1	P3	P4	6,9"	6,2"
P3	P4	P7	-1,1"	1,5"
P4	P7	P6	4,5"	2,4"
P7	P6	P5	-2,4"	-4,0"
P6	P5	P2	-4,1"	0,3"
P5	P2	P1	-8,7"	-6,6"

Table 13. Results for comparing adjusted horizontal distances.

Station	Foresight	360° Prism - Circular Prism (mm)	360° Prism - Reflective Sheet (mm)
P1	P3	0	-1
P3	P4	-1	-2
P4	P7	-1	-1
P7	P6	-1	-3
P6	P5	0	2
P5	P2	-1	-2
P2	P1	0	-2

Table 14. Results for comparing adjusted coordinates.

Station	360° Prism and Circular Prism		360° Prism and Reflective Sheet	
	delta X (m)	delta Y (m)	delta X (m)	delta Y (m)
P1	0,0000	0,0000	0,0000	0,0000
P3	0,0000	-0,0001	0,0000	-0,0007
P4	0,0011	-0,0012	0,001	-0,0024
P7	0,0045	-0,0023	0,0056	-0,0031
P6	0,0029	-0,0014	0,0040	-0,0008
P5	0,0014	-0,0015	0,0028	-0,0035
P2	-0,0002	-0,0006	0,0000	-0,0022

In relation to the information provided by the RTS manufacturer, with regard to angles, no estimative of precision was found greater than the value of 5" reported by the manufacturer, as can be seen in table 8.

Regarding the distances, for the 360° prism, no significant differences were found in relation to those specified by the RTS manufacturer, as the highest precision estimates were ±2,6mm for the P4-P7 and P5-P2 alignments, which are those with the longest traverse lengths, with 121,629m and 87,453m respectively. For the circular prism, the precision estimates for all distances after adjustment were ±2,9mm, which does not mean a discrepant value, however, as this prism is not an original accessory from the same RTS manufacturer, the difference between the estimates of precision, even if very small, may originate from this fact. The same reasoning applies to the reflective sheet, however, we add the fact that, in this case, the RTS was used manually, as the reflective sheet was not automatically detected

by the equipment in the same way that the two prisms were. It is probably for these reasons that the precision estimates for the reflective sheet for all distances were ±3mm.
Another result that can be obtained is in relation to the scale of the base, that is, in relation to the measurements of the horizontal distances between the pillars, in pairs, according to the order in which they are found in the field. Namely, the distances are as follows: P1-P2, P2-P3, P3-P4, P4-P5, P5-P6, and P6-P7. Therefore, based on the adjusted coordinates, these distances were calculated and are found in Table 15, for the three targets, and the comparisons between the distances for the 360° prism and the other two targets are in table 16.

Table 15. Results for baseline horizontal distances from the adjusted coordinates.

Alignment		Distances (m)		
		360° Prism	Circular Prism	Reflective Sheet
P1	P2	8,3008	8,3014	8,3030
P2	P3	4,4380	4,4375	4,4365
P3	P4	33,1248	33,1259	33,1265
P4	P5	49,8904	49,8907	49,8915
P5	P6	39,4802	39,4801	39,4775
P6	P7	32,2582	32,2591	32,2605

Table 16. Results for comparing baseline horizontal distances.

Alignment		Distances differences	
		360° Prism - Circular Prism (mm)	360° Prism - Reflective Sheet (mm)
P1	P2	-0,6	-2,2
P2	P3	0,5	1,5
P3	P4	-1,1	-1,7
P4	P5	-0,3	-1,1
P5	P6	0,1	2,7
P6	P7	-0,9	-2,3

The biggest difference found for the comparison between the distances for the 360° prism and the circular prism was -1.1 mm for the alignment between pillars P3 and P4. This difference does not exceed the precision estimates for the distances involved, as shown in table 9. The same applies to the comparison between the 360° prism and the reflective sheet, as the largest difference found was 2.7 mm, which also does not exceed the precision estimates of the distances involved, provided in table 9.
A suitable analysis, based on the calculated distances between the pillars, can be made through a comparison with the same measurements that were presented in [22], that is, in Garnés, Seixas e Silva (2014). In this way, table 17 was created, which shows the distances found in this work and in [22], with the respective differences.

Table 17. Comparison of horizontal distances to the 360° prism in relation to Garnés, Seixas e Silva (2014).

Alignment		Distances (m)		Difference (mm)
		360° Prism	Garnés, Seixas e Silva (2014)	
P1	P2	8,3008	8,3000	0,8
P2	P3	4,4380	4,4390	-1
P3	P4	33,1248	33,1270	-2,2

P4	P5	49,8904	49,8900	0,4
P5	P6	39,4802	39,4810	-0,8
P6	P7	32,2582	32,2580	0,2

According to table 17, the biggest difference found was -2.2mm, for the alignment between pillars P3 and P4. Considering that the work carried out previously used a Topcon total station, model GPT3200, which has a linear precision of ±5 mm +5 ppm (parts per million) [22], the results of the comparisons are compatible.

IV. CONCLUSIONS

A study on closed traverses, measured with a Topcon GT-605 RTS, for three different types of reflective surfaces (360° prism, circular prism, and reflective sheet), at the calibration baseline of the Federal University of Pernambuco was carried out. After the positive results of the statistical analyzes for horizontal angles, referring to the Shapiro-Wilk normality test and the t-test, the field data were subjected to traverse calculations using the least squares method. Once, for each of three traverses, with the results for the adjusted observations and parameters, with respective precision estimates, it was possible to carry out some analyzes and comparisons.

In this way, the adjusted horizontal angles, the adjusted horizontal distances and the adjusted coordinates were compared, always using the 360° prism as a reference, as this accessory originally accompanies the RTS used. For horizontal angles, in comparisons, the most significant differences were observed at pillars P2 and P3, that was -8,7" and 6,9" respectively, for the 360° prism and circular prism; this could be due mainly to the relatively short distances measured from these stations to both the backsight and foresight, as can be seen in table 9.

In terms of distances, in comparisons, only one measurement exceeded the equipment's linear precision. This was at station P7 for the reflective sheet, in comparison with the 360° prism, with a value of 3 mm. Nonetheless, this difference did not surpass the precision estimation for the reflective sheet, which was also 3 mm, as can be seen in table 9.

With the adjusted coordinates in table 11, it was possible to estimate the distances between the pillars, in pairs. Such calculations were made, and the results were compared with the results of a previous study, revealing that the differences found are within the precisions of the equipment used in the two studies, as can be seen in table 17.

As future work on the same baseline, a precision geometric leveling can be carried out so that the heights of the pillars can be analyzed and/or compared with those arising from a trigonometric leveling with a total station, for example.

Furthermore, another application in which the methodology proposed in this work can be used refers to the study of alignments of engineering structures. This statement is justified because these surveys are essential across a wide range of engineering applications, from the tooling industry to measuring deformations in long engineering structures, and the conventional surveying techniques that use total stations in an adequate coordinate system, among the other methods, can be employed [23].

ACKNOWLEDGEMENTS

The authors would like to thank the Department of Cartographic Engineering of the Federal University of Pernambuco, for providing the equipment and the technical infrastructure used for the acquisition of field data.

REFERENCES

[1]. S. Gopi, R. Sathikumar, N. Madhu: Advanced Surveying. Second Edition. Uttar Pradesh: Pearson India Education Services Pvt. Ltd, 2018.

[2]. L. Nadolinetz, E. Levin, D. Akhmedov: Surveying Instruments and Technology. CRC Press. Boca Raton: 2017.

[3]. H. Simas, R. Di Gregorio, R. Simoni, M. Gatti: Parallel Pointing Systems Suitable for Robotic Total Stations: Selection, Dimensional Synthesis, and Accuracy Analysis. Machines 2024, 12, 54. doi.org/10.3390/machines12010054.

[4]. J. Uren, B. Price: Surveying for Engineers. Fifth edition. New York: Palgrave Macmillan, 2010.

[5]. N. W. J. Hazelton: Levelling and Total Stations. In: Surveying and Geomatics Engineering: principles, technologies, and applications, edited by D. T. Gillins, M. L. Dennis, A. Y. Reston: 2022. American Society of Civil Engineers, ASCE.

[6]. G. Youyi, J. Lixing, W. Ancheng, W. Li, O. Yangwen: Error Analysis of Calibration Length Baseline based on μ-base Distance Meter. IOP Conf. Series: Earth and Environmental Science 237 (2019) 032022.

[7]. S. Saadati, M. Abbasi, S. Abbasy, A. Amiri-Simkooei: Geodetic calibration network for total stations and GNSS receivers in sub-kilometer distances with sub-millimeter precision. Measurement 141 (2019), 258–266.

[8]. D. M. Zakari, A. Aliyu: Establishment of Baseline using Electronic Distance Measurement. IOSR Journal Of Environmental Science, Toxicology And Food Technology (IOSR-JESTFT), e-ISSN: 2319-2402, p- ISSN: 2319-2399. Volume 8, Issue 1 Ver. IV (Feb. 2014), pp 79-85.

[9]. NGS: Electronic Distance Measuring Instrumentation Calibration Baseline Program Policy. NOAA's National Geodetic Survey - NGS, 2017.

[10]. A. Buga, R. Birvydiene, R. Kolosovskis, B. Krikstaponis, R. Obuchovski, E. Parseliunas, R. Putrimas, D. Slikas: Analysis of the calibration quality of the Kyviskes Calibration Baseline. Acta Geod Geophys (2016) 51:505–514.

[11]. A. Buga, R. Putrimas, D. Slikas, J. Jokela: Kyviskes Calibration Baseline: measurements and improvements analysis. The 9th Conference Environmental Engineering. Selected Papers, 22–23 May 2014, Vilnius, Lithuania Article number: enviro.2014.195.

[12]. G. E. V. Becerra, R. A. Bennett, M. C. Chávez, M. E. T Soto, J. R. Camacho: Short Baseline Calibration using GPS and EDM Observations. Geofísica International 54-3: 255-266, 2015.

[13]. B. Bozic, H. Fan, Z. Milosavljevic: Establishment of the MGI EDM calibration baseline. Survey Review, 2013, Vol 45, n° 331.

[14]. I. R. Junior, A. Seixas, S. J. A. Garnés: Alignment Study of an Electronic Distance Measuring Instruments Calibration Baseline Using Total Station. International Journal of Advances in Engineering & Technology, April, 2024, Vol. 17, Issue 2, pp. 90-97.

[15]. F. S. Barbosa: A Escala do Basímetro Linear. Aplicação: Base Multipilar da UFPE. Dissertação de Mestrado apresentada ao programa de pós graduação em Ciências Geodésicas e Tecnologias da Geoinformação da Universidade Federal de Pernambuco. Recife, 2009.

[16]. TOPCON: Instruction Manual - Geodetic Total Station GT series, 2022.

[17]. H. Kahmen, W. Faig: Surveying. Berlin: de Gruyter, 1988.

[18]. M. F. Triola: Elementary Statistics. 14th edition. Hoboken: Pearson, 2022.

[19]. S. J. A. Garnés: AstGeoTop. Software. Módulo Análise Estatística. Recife-PE: Departamento de Engenharia Cartográfica. Universidade Federal de Pernambuco, 2024.

[20]. S. J. A. Garnés: AstGeoTop. Software. Módulo Levantamento Planimétrico Recife-PE: Departamento de Engenharia Cartográfica. Universidade Federal de Pernambuco, 2024.

[21]. C. D. Ghilani: Adjustment Computations: Spatial Data Analysis. Sixth edition. Hoboken: John Wiley & Sons, 2017.

[22]. S. J. A. Garnés, A. Seixas, T. F. Silva: Análise do alinhamento da base de calibração multi pilar do LAMEP/UFPE com proposição de modelo de correção. V Simpósio Brasileiro de Ciências Geodésicas e Tecnologias da Geoinformação Recife - PE, 12- 14 de Novembro de 2014.

[23]. J. O. Ogundare: Precision Surveying: the principles and geomatics practice. Hoboken: John Wiley & Sons, 2016.

AUTHORS

Isaac Ramos Junior - is a Master's student in Geodetic Sciences and Geoinformation Technologies at Federal University of Pernambuco, Brazil.

Andrea de Seixas is an Associate Professor at the Department of Cartographic Engineering at the Federal University of Pernambuco, Brazil.

Sílvio Jacks dos Anjos Garnés has a Doctorate in Geodetic Sciences at Federal University of Paraná. He is an Associate Professor at the Department of Cartographic Engineering at the Federal University of Pernambuco, Brazil.